

Partition of friction heat between sliding semispaces due to adhesion-deformational heat generation

Oleksii Nosko

Department of Mechanical Engineering, Saitama University
255 Shimo-Okubo, Sakura-ku, Saitama-shi, Saitama, 338-8570, Japan
tel.: +81 48 858 3730, fax: +81 48 858 3771
nosko_a@mail.ru

Analytical expressions of heat-partition coefficient and contact temperatures for two sliding semispaces with account for adhesion-deformational heat generation and contact heat exchange have been obtained. The rate of deformational heat generation is assumed to decay exponentially with increase of distance from the interface. It has been shown that heat-generation configuration and the intensity of contact heat exchange have impact on heat partition only within a transient interval. The features of perfect thermal contact have been analyzed. Perfect thermal contact implies variation of heat partition in time. Heat partition and contact temperature for a semispace, sliding over a semispace with a constant temperature, have been studied. Adhesion-deformational heat generation results in a change of the direction of surface heat flow.

Keywords: friction heat partition, imperfect thermal contact, sliding contact temperature.

1. Introduction

It is well recognized that one of the most important factors in sliding systems is temperature at the interface. This influences the friction processes in a variety of ways. Generally, temperature has effects on friction coefficient, mechanical properties, such as elastic modulus and hardness, wear rate, etc. Therefore, an estimate of its magnitude is often required.

Most of the studies on temperature at sliding interfaces have been based on the flash temperature theory [1–3] where perfect thermal contact, i.e. heat balance and temperature continuity, is assumed in the microscopic regions of roughness asperities interaction. Heat-partition coefficient α_f has been introduced to divide friction heat between the sliding bodies. α_f enables defining a boundary thermal condition in the form of heat-flow rate q_i per unit surface area of each i -th body, $i \in \{1, 2\}$, as illustrated in Fig.1(a). A sum $q_1 + q_2$ is equal to specific power q of friction-heat generation.

For simplicity, temperature continuity at macroscopic interface is sometimes assumed [4]. This implies the equality of the temperatures T_i of the sliding bodies, as shown in Fig.1(b).

In reality, at macroscopic interface $T_1 \neq T_2$, i.e. thermal interaction is imperfect, and contact heat exchange is observed [5]. Its intensity is characterized by a value R of thermal contact resistance or by contact heat exchange coefficient $\gamma = 1/R$. One of the simplest frictional thermal models considering R is depicted in Fig.1(c) [6]. According to experimental data [7], contact heat exchange can result in a considerable variation of α_f in the course of friction. Therefore, α_f should be generally treated as not a parameter but a variable quantity.

It is common knowledge [8] that dry friction has two basic components: the interfacial bonds between the bodies (adhesive component) and the deformation of roughness asperities and neighboring volumes of materials (deformational component). Both components are related to generation of heat. Adhesive component contributes to heat generation at the sliding surfaces, while deformational one contributes to volumetric heat generation in the subsurface layers. A fraction ψ of friction heat released due to the adhesive mechanism may be different in relation to friction materials. For metals, ψ is considered to be small, e.g. for copper / steel pair $\psi < 0.15$, i.e. adhesive component provides less than 15% of friction heat [9].

Heat generation in the subsurface layers is induced mainly by plastic deformation. Volumetric rate ω of heat generation depends on the distance x from the interface and cannot be measured directly. However, a distribution $\omega(x)$ is supposed to be of the same profile as plastic-deformation distribution [10]. That deformation is estimated through the observation of a transverse section of a worn surface. Experiments show [11, 12] that plastic displacement δ diminishes rapidly with x . For approximation of $\delta(x)$, the exponential is sometimes used [13–15]. As an example, a profile $\delta(x)$ in a copper specimen after sliding against a steel slider is presented in Fig.2 [10].

A model [16, 17] depicted in Fig.1(d) has been developed to take into account the deformational component of heat generation. The parameters of the model are heat-generation coefficient α and γ . The coefficient α specifies a fraction of friction heat which is generated at the surface and in the subsurface layer of the first body.

There is a principal difference between α_f and α : the former means a partition of friction heat, whereas the latter specifies a partition of heat-generation rate between the sliding bodies. When using the models Figs.1(b),(c),(d), α_f is a priori unknown.

A number of analytical studies on temperatures in sliding systems have been conducted. We mention non-stationary problems in which the bodies are represented in the form of the semispaces or geometrically generalized systems (layer–semispace, plane-parallel layers, semispace–layer–semispace). A classical solution for the semispaces with perfect thermal contact Fig.1(b) has been provided in [4]. Imperfect thermal contact for the semispaces and for plane-parallel layers has been thoroughly studied: with account for γ [18, 19] due to the model Fig.1(c); with account for α and γ [20, 21] due to the model Fig.1(d). There have been also obtained the solutions for a layer–semispace system [22, 23] and for the semispaces where one of them is homogeneous and the other is a semi-infinite foundation covered by a layer [24].

The solutions referred above assume heat generation localized at the interface. In some cases the validity of this assumption is subject to question.

Temperature in a semispace with a moving band heat source has been analyzed [25]. It was shown that maximum surface temperatures obtained for the distributions $\omega(x)$, similar to the exponential approximation in Fig.2, are noticeably lower than the maximum temperature corresponding to localized heat source. Low surface temperatures may be observed in the real friction systems when the deformational component is considerable [26].

Temperature distribution in a titanium sample, sliding over a molybdenum braking disk, has been studied experimentally [27]. It was found that a subsurface temperature can exceed the temperature at the surface in the course of friction. Since the subsurface layer of the sample was subjected to large plastic deformations, the effect of $\omega(x)$ on the temperature distribution was concluded to be significant.

According to these reports, generation of friction heat may be essentially volumetric and in this case $\omega(x)$ cannot be neglected. In the present work the model Fig.1(d) is modified to take into account $\omega(x)$. For simplicity, $\omega(x)$ is defined by the exponential. Analytical study of heat partition and contact temperatures for the sliding semispaces is conducted. α_f is expressed as a time function depending on the thermophysical properties of the semispaces, the coefficients α , γ and ψ_i for each i -th semispace. The features of perfect thermal contact for adhesive and adhesion-deformational heat generation are analyzed. The influence of heat-generation configuration on heat partition and contact temperature for a semispace, sliding over a constant-temperature semispace, is studied.

2. Heat-generation coefficient α

There are several theoretical approaches to determine α .

A model [28, 29] depicted in Fig.1(e) corresponds to the case of pure adhesive heat generation, i.e. $\psi_1 = \psi_2 = 1$. The roughness of each i -th body is characterized by a microscopic thermal resistance R_i . From the condition of identity of the models in Figs.(d) and (e), it follows that

$$\alpha = \frac{R_2}{R_1 + R_2}; \quad \gamma = \frac{1}{R_1 + R_2}$$

Thermomechanical approach has been reported [16]. Roughness asperities of each i -th body are represented as a set of equal spherical segments with a radius r_i . Adhesive and deformational interactions within a single couple of asperities are studied. α is obtained as a complicated expression which includes mechanical, thermophysical and geometrical characteristics. We restrict ourselves to the consideration of two limiting cases

$$\alpha|_{\psi_1=\psi_2=1} = \left(1 + \frac{c_2 k_2}{c_1 k_1} \left(\frac{r_2 E_1 (1 - \nu_2^2)}{r_1 E_2 (1 - \nu_1^2)} \right)^{2/3} \right)^{-1};$$

$$\alpha|_{\psi_1=\psi_2=0} = \left(1 + \left(\frac{r_1}{r_2} \right)^{1/3} \left(\frac{E_1 (1 - \nu_2^2)}{E_2 (1 - \nu_1^2)} \right)^{2/3} \right)^{-1}$$

where c_i is specific heat capacity; k_i is thermal diffusivity coefficient; E_i is elastic modulus; ν_i is Poisson's ratio.

Sliding between a body with periodic asperities ($i = 1$) and a perfectly smooth body ($i = 2$) has been analyzed in [30, 31]. For each i -th body, friction heat is assumed to be generated in the subsurface layer with a thickness d_i due to some distribution $\omega_i(x)$. Adhesive heat generation is neglected, i.e. $\psi_1 = \psi_2 = 0$. With the preceding notation, the following expression is derived:

$$\alpha = \int_0^{d_1} \frac{R_2 + R_1 x/d_1}{R_1 + R_2} \frac{\omega_1(x)}{q} dx + \int_0^{d_2} \frac{R_2 (1 - x/d_2)}{R_1 + R_2} \frac{\omega_2(x)}{q} dx$$

3. Problem definition

We consider two semispaces. Each i -th semispaces occupies a domain $(-1)^{i+1} x > 0$ and possesses a thermal conductivity coefficient K_i and a thermal diffusivity coefficient k_i . At initial moment $t = 0$ the temperature of the semispaces is T_0 . Starting from this moment the semispaces slide relative to each other in the plane $x = 0$ so that there is generation of friction heat with a specific power q .

It should be noted that in the present formulation the quantity x is a coordinate. Accordingly, a distance from the interfacial plane is equal to x for the first semispaces and $|x|$ for the second one.

Let us assume the following. A fraction α of friction heat is generated in the first semispaces, while the complementary fraction $(1 - \alpha)$ is generated in the second one. For each i -th semispaces, a fraction ψ_i of relevant heat is released in the plane $x = 0$ due to the adhesive mechanism and the reminder $(1 - \psi_i)$ is released in the volume through the deformational mechanism, as shown in Fig.1(f). The volumetric rates ω_i of heat generation are distributed by the exponential law

$$\omega_1 = \frac{\alpha(1 - \psi_1)q}{h_1} \exp\left(-\frac{x}{h_1}\right), \quad x > 0;$$

$$\omega_2 = \frac{(1 - \alpha)(1 - \psi_2)q}{h_2} \exp\left(\frac{x}{h_2}\right), \quad x < 0$$

where h_i is effective thickness of the i -th subsurface layer determined from plastic-deformation distribution. In the plane $x = 0$ there is contact heat exchange between the semispaces with intensity specified by γ .

In agreement with the mentioned assumptions, the temperatures T_i in the semispaces are governed by the equations

$$\begin{aligned} \frac{\partial T_1}{\partial t} &= k_1 \frac{\partial^2 T_1}{\partial x^2} + \frac{\alpha(1 - \psi_1)k_1 q}{h_1 K_1} \exp\left(-\frac{x}{h_1}\right), \quad x > 0, \quad t > 0; \\ \frac{\partial T_2}{\partial t} &= k_2 \frac{\partial^2 T_2}{\partial x^2} + \frac{(1 - \alpha)(1 - \psi_2)k_2 q}{h_2 K_2} \exp\left(\frac{x}{h_2}\right), \quad x < 0, \quad t > 0; \\ T_1|_{t=0} &= T_2|_{t=0} = T_0; \\ -K_1 \frac{\partial T_1}{\partial x} \Big|_{x=0} &= \alpha\psi_1 q - \gamma(T_1 - T_2)|_{x=0}; \\ K_2 \frac{\partial T_2}{\partial x} \Big|_{x=0} &= (1 - \alpha)\psi_2 q + \gamma(T_1 - T_2)|_{x=0}; \\ \frac{\partial T_1}{\partial x} \Big|_{x \rightarrow +\infty} &= \frac{\partial T_2}{\partial x} \Big|_{x \rightarrow -\infty} = 0 \end{aligned} \quad (1)$$

All four components of heat generation for both semispaces satisfy the heat-balance condition

$$\alpha\psi_1 q + \int_0^{+\infty} \frac{\alpha(1 - \psi_1)q}{h_1} \exp\left(-\frac{x}{h_1}\right) dx + (1 - \alpha)\psi_2 q + \int_{-\infty}^0 \frac{(1 - \alpha)(1 - \psi_2)q}{h_2} \exp\left(\frac{x}{h_2}\right) dx = q$$

After introducing dimensionless coordinate $\xi = x/h_1$, dimensionless time variable (Fourier number) $Fo = k_1 t/h_1^2$, dimensionless temperatures $\vartheta_i = K_1(T_i - T_0)/qh_1$, $\Lambda = K_1/K_2$, $\chi = k_2/k_1$, $H = h_2/h_1$, $B = \gamma h_1/K_1$, Eq.(1) is represented as

$$\begin{aligned} \frac{\partial \vartheta_1}{\partial Fo} &= \frac{\partial^2 \vartheta_1}{\partial \xi^2} + \alpha(1 - \psi_1) \exp(-\xi), \quad \xi > 0, \quad Fo > 0; \\ \frac{\partial \vartheta_2}{\partial Fo} &= \chi \frac{\partial^2 \vartheta_2}{\partial \xi^2} + (1 - \alpha)(1 - \psi_2) \frac{\Lambda \chi}{H} \exp\left(\frac{\xi}{H}\right), \quad \xi < 0, \quad Fo > 0; \\ \vartheta_1|_{Fo=0} &= \vartheta_2|_{Fo=0} = 0; \\ -\frac{\partial \vartheta_1}{\partial \xi} \Big|_{\xi=0} &= \alpha\psi_1 - B(\vartheta_1 - \vartheta_2)|_{\xi=0}; \\ \Lambda^{-1} \frac{\partial \vartheta_2}{\partial \xi} \Big|_{\xi=0} &= (1 - \alpha)\psi_2 + B(\vartheta_1 - \vartheta_2)|_{\xi=0}; \\ \frac{\partial \vartheta_1}{\partial \xi} \Big|_{\xi \rightarrow +\infty} &= \frac{\partial \vartheta_2}{\partial \xi} \Big|_{\xi \rightarrow -\infty} = 0 \end{aligned} \quad (2)$$

The problem defined by Eq.(2) includes special cases:

- perfect thermal contact at $B \rightarrow +\infty$;
- absence of contact heat exchange at $B = 0$;
- pure adhesive heat generation at $\psi_1 = \psi_2 = 1$;

- pure deformational heat generation at $\psi_1 = \psi_2 = 0$;
- contact with constant-temperature semispace at $\chi \rightarrow 0$.

4. Problem solution

We apply Laplace integral transform \mathcal{L} to Eq.(2) and obtain the images $\vartheta_{Li}(\xi, s) = \mathcal{L}[\vartheta_i(\xi, Fo)]$ as follows

$$\begin{aligned} \vartheta_{L1} &= \frac{\alpha(1-\psi_1)}{s(s-1)} \exp(-\xi) + \left(\frac{\alpha\psi_1}{s(\sqrt{s+B(1+\mu)})} + \frac{(\alpha\psi_1+(1-\alpha)\psi_2)B\mu}{s\sqrt{s}(\sqrt{s+B(1+\mu)})} \right. \\ &\quad \left. - \frac{\alpha(1-\psi_1)(1+B)}{s(s-1)(\sqrt{s+B(1+\mu)})} - \frac{\alpha(1-\psi_1)B\mu}{s\sqrt{s}(s-1)(\sqrt{s+B(1+\mu)})} + \frac{(1-\alpha)(1-\psi_2)B\mu\lambda}{s\sqrt{s}(\sqrt{s+\lambda})(\sqrt{s+B(1+\mu)})} \right) \exp(-\xi\sqrt{s}); \\ \vartheta_{L2} &= \frac{(1-\alpha)(1-\psi_2)\mu\lambda}{s(s-\lambda^2)} \exp\left(\frac{\xi}{H}\right) + \left(\frac{(1-\alpha)\psi_2\mu}{s(\sqrt{s+B(1+\mu)})} + \frac{(\alpha\psi_1+(1-\alpha)\psi_2)B\mu}{s\sqrt{s}(\sqrt{s+B(1+\mu)})} \right. \\ &\quad \left. - \frac{(1-\alpha)(1-\psi_2)(B\mu+\lambda)\mu\lambda}{s(s-\lambda^2)(\sqrt{s+B(1+\mu)})} - \frac{(1-\alpha)(1-\psi_2)B\mu\lambda^2}{s\sqrt{s}(s-\lambda^2)(\sqrt{s+B(1+\mu)})} + \frac{\alpha(1-\psi_1)B\mu}{s\sqrt{s}(\sqrt{s+1})(\sqrt{s+B(1+\mu)})} \right) \exp\left(\xi\sqrt{\frac{s}{\chi}}\right) \end{aligned} \quad (3)$$

where s is transform parameter; $\lambda = \sqrt{\chi}/H$; $\mu = \Lambda\sqrt{\chi}$.

By setting $\xi = 0$ in Eq.(3) and using the known inverse Laplace transforms [4]

$$\begin{aligned} \mathcal{L}^{-1}\left[\frac{a^2}{s(s-a^2)}\right] &= \exp(a^2 Fo) - 1; \\ \mathcal{L}^{-1}\left[\frac{b}{s(\sqrt{s+b})}\right] &= 1 - \exp(b^2 Fo) \operatorname{erfc}(b\sqrt{Fo}); \\ \mathcal{L}^{-1}\left[\frac{b^2}{s\sqrt{s}(\sqrt{s+b})}\right] &= \frac{2b\sqrt{Fo}}{\sqrt{\pi}} + \exp(b^2 Fo) \operatorname{erfc}(b\sqrt{Fo}) - 1; \\ \mathcal{L}^{-1}\left[\frac{a^2 b}{s(s-a^2)(\sqrt{s+b})}\right] &= \frac{b \exp(a^2 Fo) (b-a+a \operatorname{erfc}(a\sqrt{Fo}))}{b^2-a^2} - \frac{a^2 \exp(b^2 Fo) \operatorname{erfc}(b\sqrt{Fo})}{b^2-a^2} - 1; \\ \mathcal{L}^{-1}\left[\frac{a^2 b^2}{s\sqrt{s}(s-a^2)(\sqrt{s+b})}\right] &= 1 - \frac{2b\sqrt{Fo}}{\sqrt{\pi}} - \frac{b^2 \exp(a^2 Fo) (a-b+b \operatorname{erfc}(a\sqrt{Fo}))}{a(b^2-a^2)} + \frac{a^2 \exp(b^2 Fo) \operatorname{erfc}(b\sqrt{Fo})}{b^2-a^2}; \\ \mathcal{L}^{-1}\left[\frac{ab}{s\sqrt{s}(\sqrt{s+a})(\sqrt{s+b})}\right] &= \frac{2\sqrt{Fo}}{\sqrt{\pi}} - \frac{a+b}{ab} + \frac{b \exp(a^2 Fo) \operatorname{erfc}(a\sqrt{Fo})}{a(b-a)} - \frac{a \exp(b^2 Fo) \operatorname{erfc}(b\sqrt{Fo})}{b(b-a)} \end{aligned}$$

we derive θ_i and α_f in the form

$$\begin{aligned} \theta_1 &= \vartheta_1|_{\xi=0} = \frac{2\mu}{\sqrt{\pi}(1+\mu)} \sqrt{Fo} - \frac{\alpha(1-\psi_1)(1-B\mu)}{1-B(1+\mu)} \Psi(Fo) + \frac{(1-\alpha)(1-\psi_2)B\mu}{\lambda(\lambda-B(1+\mu))} \Psi(\lambda^2 Fo) \\ &\quad + \frac{1}{1+\mu} \left(\frac{1}{B(1+\mu)} + \frac{\alpha(1-\psi_1)}{1-B(1+\mu)} - \frac{(1-\alpha)(\lambda-B(1+\psi_2\mu))}{B(\lambda-B(1+\mu))} \right) \Psi(B^2(1+\mu)^2 Fo); \\ \theta_2 &= \vartheta_2|_{\xi=0} = \frac{2\mu}{\sqrt{\pi}(1+\mu)} \sqrt{Fo} + \frac{\alpha(1-\psi_1)B\mu}{1-B(1+\mu)} \Psi(Fo) - \frac{(1-\alpha)(1-\psi_2)(\lambda-B)\mu}{\lambda(\lambda-B(1+\mu))} \Psi(\lambda^2 Fo) \\ &\quad + \frac{1}{B(1+\mu)} \left(\frac{B-(1-\alpha)(1+\mu)\lambda}{B(1+\mu)} + \frac{(1-\alpha)((\lambda-B)^2-\psi_2 B^2 \mu^2)}{B(\lambda-B(1+\mu))} - \frac{\alpha(1-B(1+\psi_1\mu))}{1-B(1+\mu)} \right) \Psi(B^2(1+\mu)^2 Fo); \\ \alpha_f &= \alpha - B(\theta_1 - \theta_2) = \alpha + \frac{\alpha(1-\psi_1)B}{1-B(1+\mu)} \Psi(Fo) - \frac{(1-\alpha)(1-\psi_2)B\mu}{\lambda-B(1+\mu)} \Psi(\lambda^2 Fo) \\ &\quad - \frac{1}{1+\mu} \left(\frac{(1-\alpha)\lambda}{B} + \frac{\alpha(1-\psi_1 B(1+\mu))}{1-B(1+\mu)} - \frac{(1-\alpha)((\lambda-B)\lambda-\psi_2 B^2 \mu(1+\mu))}{B(\lambda-B(1+\mu))} \right) \Psi(B^2(1+\mu)^2 Fo) \end{aligned} \quad (4)$$

where $\operatorname{erfc}(\cdot)$ is complementary error function; a and b are positive numbers; $\Psi(z) = 1 - \exp(z) \operatorname{erfc}(\sqrt{z})$.

The function Ψ increases monotonically from zero value at $z = 0$ to the unit at infinite point $z = +\infty$ (Table 1).

Table 1. Threshold values of the function Ψ and its argument, $\Psi_s = \Psi(z_s)$

Ψ_s	0	0.1	0.2	0.3	0.4	0.5	0.6	0.7
z_s	0	0.009270	0.04465	0.1242	0.2823	0.5915	1.226	2.692
Ψ_s	0.8	0.9	0.95	0.96	0.97	0.98	0.99	1
z_s	7.037	30.85	126.3	197.9	352.7	794.8	3182	$+\infty$

Thus, θ_i and α_f are represented as analytical expressions depending on 6 dimensionless parameters, namely, α , ψ_1 , ψ_2 , λ , B and μ . The parameters α , ψ_1 , ψ_2 and λ define heat-generation configuration. B is dimensionless contact heat exchange coefficient. μ is the ratio of thermal effusivities of the semispaces.

It should be mentioned that Eq.(4) can be obtained as a superposition of a solution for the localized heat generation due to the model Fig.1(d) and a solution for the volumetric heat generation with exponentially decaying $\omega_i(x)$. These solutions have been reported, for instance, in [20].

5. Transient process

For small values of Fo it is true

$$\begin{aligned}\theta_1 &= \frac{2\alpha\psi_1}{\sqrt{\pi}}\sqrt{\text{Fo}} + (\alpha - \alpha\psi_1(1+B) + (1-\alpha)\psi_2B\mu)\text{Fo} + O(\text{Fo}^{3/2}); \\ \theta_2 &= \frac{2(1-\alpha)\psi_2\mu}{\sqrt{\pi}}\sqrt{\text{Fo}} + \mu((1-\alpha)\lambda + \alpha\psi_1B - (1-\alpha)\psi_2(B\mu + \lambda))\text{Fo} + O(\text{Fo}^{3/2}); \\ \alpha_f &= \alpha + O(\text{Fo}^{1/2})\end{aligned}\quad (5)$$

At $\text{Fo} \rightarrow 0$ the temperatures θ_i rise as $\sqrt{\text{Fo}}$. However, if pure deformational heat generation occurs, i.e. $\psi_i = 0$, they are proportional to Fo.

When $\text{Fo} \rightarrow +\infty$, the quantities under study tend to

$$\theta_1 = \theta_2 = \frac{2\mu}{\sqrt{\pi}(1+\mu)}\sqrt{\text{Fo}}; \quad \alpha_f = \frac{\mu}{1+\mu}\quad (6)$$

At large values of Fo the temperatures θ_i as well as α_f are independent of heat-generation configuration and B . They exhibit behavior intrinsic to the sliding semispaces with perfect thermal contact and pure adhesive heat generation [4].

Eq.(4) describes a transient process [8, 16]: friction is initially inequilibrium and heat partition is governed by the properties of rough surfaces, as indicated by Eq.(5); eventually friction tends to equilibrium state Eq.(6) where heat partition is due to thermophysical properties of the sliding bodies. α_f includes three variable terms which change in accordance with the functions $\Psi(\text{Fo})$, $\Psi(\lambda^2\text{Fo})$ and $\Psi(B^2(1+\mu)^2\text{Fo})$, respectively. If the slowest of them is accepted as governing, then saturation of α_f to a level Ψ_s occurs at the moment

$$\text{Fo}_s = \frac{z_s}{\min\{1, \lambda^2, B^2(1+\mu)^2\}}$$

Hence, it is advisable to use Eq.(4) for the transient interval $\text{Fo} \leq \text{Fo}_s$. For $\text{Fo} > \text{Fo}_s$ the simpler Eq.(6) can be used.

6. Perfect thermal contact

Generally, the temperatures θ_i are different. It is explained by that a capacity of each semispace to remove heat from the interfacial zone does not correspond to the amount of heat generated in this semispace [32]. Nevertheless, there exist certain conditions under which a balance between the heat generation and the heat removal is established and thermal contact becomes perfect. These conditions are of special interest.

If pure adhesive heat generation occurs, i.e. $\psi_1 = \psi_2 = 1$, then

$$\begin{aligned}\theta_1 &= \frac{2\mu}{\sqrt{\pi}(1+\mu)}\sqrt{\text{Fo}} - \frac{\mu - \alpha(1+\mu)}{B(1+\mu)^2} \Psi(B^2(1+\mu)^2\text{Fo}); \\ \theta_2 &= \frac{2\mu}{\sqrt{\pi}(1+\mu)}\sqrt{\text{Fo}} + \frac{\mu(\mu - \alpha(1+\mu))}{B(1+\mu)^2} \Psi(B^2(1+\mu)^2\text{Fo}); \\ \alpha_f &= \alpha + \left(\frac{\mu}{1+\mu} - \alpha\right) \Psi(B^2(1+\mu)^2\text{Fo})\end{aligned}\quad (7)$$

Identical equality of θ_i in Eq.(7) is valid in the case $\alpha = \mu/(1+\mu)$ or in the case $B \rightarrow +\infty$. In both these cases Eq.(7) transforms into Eq.(6) where heat partition occurs due to thermal-effusivities proportion. Consequently, perfect thermal contact Eq.(6) has two interpretations:

- at $\alpha = \mu/(1+\mu)$ friction heat is initially released so that $\theta_1 = \theta_2$ and the coefficient B , whatever it is, has no effect on thermal processes;

- at $B \rightarrow +\infty$ heat-generation disproportion $\alpha \neq \mu/(1 + \mu)$ is neutralized by the «ability» of the interface to equalize the temperatures θ_i immediately.

Now we consider a general case of heat generation involving deformational component.

If there is no contact heat exchange, i.e. $B \rightarrow 0$, it is true

$$\begin{aligned}\theta_1 &= \frac{2\alpha}{\sqrt{\pi}}\sqrt{Fo} - \alpha(1 - \psi_1) \Psi(Fo); \\ \theta_2 &= \frac{2(1 - \alpha)\mu}{\sqrt{\pi}}\sqrt{Fo} - \frac{(1 - \alpha)(1 - \psi_2)\mu}{\lambda} \Psi(\lambda^2 Fo); \\ \alpha_f &= \alpha\end{aligned}\quad (8)$$

After equalizing θ_i given by Eq.(8) we obtain

$$\alpha = \left(1 + \frac{\frac{2}{\sqrt{\pi}}\sqrt{Fo} - (1 - \psi_1)\Psi(Fo)}{\mu \left(\frac{2}{\sqrt{\pi}}\sqrt{Fo} - \frac{1 - \psi_2}{\lambda} \Psi(\lambda^2 Fo) \right)} \right)^{-1}$$

from which it follows that α is constant when and only when $\lambda = 1$ and $\psi_1 = \psi_2$. Under conditions

$$\lambda = 1, \quad \psi_1 = \psi_2, \quad \alpha = \mu/(1 + \mu) \quad (9)$$

the temperatures θ_i in Eq.(4) are identically equal regardless of the value of B , that is

$$\begin{aligned}\theta_1 = \theta_2 &= \frac{\mu}{1 + \mu} \left(\frac{2}{\sqrt{\pi}}\sqrt{Fo} - (1 - \psi_1) \Psi(Fo) \right); \\ \alpha_f = \alpha &= \frac{\mu}{1 + \mu}\end{aligned}\quad (10)$$

The conditions Eq.(9) are simultaneously met for friction pairs consisting of similar materials with equal roughness parameters. Therefore, Eq.(10) should be considered as a particular case of perfect thermal contact.

There are combinations of friction pairs and sliding regimes for which contact heat exchange is intensive and hence B takes a large value. In the limiting case $B \rightarrow +\infty$ we derive

$$\begin{aligned}\theta_1 = \theta_2 &= \frac{\mu}{1 + \mu} \left(\frac{2}{\sqrt{\pi}}\sqrt{Fo} - \alpha(1 - \psi_1) \Psi(Fo) - \frac{(1 - \alpha)(1 - \psi_2)}{\lambda} \Psi(\lambda^2 Fo) \right); \\ \alpha_f = \alpha &- \frac{\alpha\psi_1}{1 + \mu} + \frac{(1 - \alpha)\psi_2\mu}{1 + \mu} - \frac{\alpha(1 - \psi_1)}{1 + \mu} \Psi(Fo) + \frac{(1 - \alpha)(1 - \psi_2)\mu}{1 + \mu} \Psi(\lambda^2 Fo)\end{aligned}\quad (11)$$

Eq.(11) describes a thermal balance when the amount of heat, supplied to each semispace as a result of heat generation and contact heat exchange, corresponds to its heat-removal capability. This balance implies α_f varying in time.

7. Contact with constant-temperature semispace

There are instances when temperature variation in one of the sliding bodies is negligible. They can be simulated by Eq.(4) with $\chi \rightarrow 0$, that is

$$\begin{aligned}\theta_1/\alpha &= \frac{1 - \psi_1}{B - 1} \Psi(Fo) - \frac{1 - \psi_1 B}{B(B - 1)} \Psi(B^2 Fo); \quad \theta_2 = 0; \\ \alpha_f/\alpha &= 1 - \frac{(1 - \psi_1)B}{B - 1} \Psi(Fo) + \frac{1 - \psi_1 B}{B - 1} \Psi(B^2 Fo)\end{aligned}\quad (12)$$

According to Eq.(12), a dimensionless rate $J = -\partial\theta_1/\partial\xi|_{\xi=0}$ of heat flow, going to the semispace across its unit surface area, takes the form

$$J/\alpha = \psi_1 - \frac{(1 - \psi_1)B}{B - 1} \Psi(Fo) + \frac{1 - \psi_1 B}{B - 1} \Psi(B^2 Fo)$$

Depending on ψ_1 there are three different cases shown in Fig.3:

- $\psi_1 = 1, J = \alpha_f$ is positive at $Fo > 0$;
- $0 < \psi_1 < 1$ ($\psi_1 = 0.5$ in Fig.3), J is positive on the interval $0 < Fo < Fo_c$ and negative at $Fo > Fo_c$;
- $\psi_1 = 0, J$ is negative at $Fo > 0$.

In general case, at $Fo = Fo_c$ surface heat flow changes its direction. Accordingly, at $Fo > Fo_c$ a temperature peak is located in the subsurface layer at some distance from the surface $\xi = 0$. The dependence of Fo_c on ψ_1 and B , determined numerically from the condition $J = 0$, is depicted in Fig.4.

Subsurface temperature peaks have been investigated in [33, 34]. It was concluded that they are feasible for the regime of deceleration, i.e. for q decreasing. The analysis above shows that they may also occur under constant q .

Effect of ψ_1 on θ_1 is illustrated in Fig.5. It is seen that θ_1 increases with ψ_1 , i.e. adhesive heat generation induces a higher contact temperature than generation of the same quantity of heat through the deformational mechanism [25].

Let us consider a maximum relative deviation ε of θ_1 caused by a change in ψ_1 :

$$\varepsilon = \frac{\theta_1|_{\psi_1=1} - \theta_1|_{\psi_1=0}}{\theta_1|_{\psi_1=0}} = \frac{B \Psi(Fo) - B \Psi(B^2Fo)}{\Psi(B^2Fo) - B \Psi(Fo)}$$

Variation range of ε is shown in Fig.6. Since B has a limited effect on ε so that

$$\frac{2}{\pi} < \frac{\varepsilon|_{B \rightarrow +\infty}}{\varepsilon|_{B \rightarrow 0}} < \frac{\pi}{4}$$

it is reasonable to use $\varepsilon_B = \varepsilon|_{B \rightarrow 0}$ as an upper-bound estimate for ε :

$$\varepsilon_B = \frac{\sqrt{\pi} \Psi(Fo)}{2\sqrt{Fo} - \sqrt{\pi} \Psi(Fo)}$$

The function ε_B monotonically decreases and approaches zero at $Fo \rightarrow +\infty$ (Table 2).

Table 2. Threshold values of the function ε_B and its argument, $\varepsilon_0 = \varepsilon_B(Fo_0)$

ε_0	1	0.9	0.8	0.7	0.6	0.5	0.4	0.3
Fo_0	1.057	1.288	1.608	2.066	2.760	3.887	5.914	10.18
ε_0	0.2	0.1	0.05	0.04	0.03	0.02	0.01	0
Fo_0	22.01	83.74	325.1	504.6	891.2	1992	7911	$+\infty$

Thus, for a specified level ε_0 of temperature deviation it is recommended to take into account the influence of ψ_1 on θ_1 within the interval $Fo \leq Fo_0$. At $Fo > Fo_0$ the ratio of the rates of heat-generation components is not important and pure adhesive heat generation can be assumed for simplicity.

8. Conclusions

Exact expressions Eq.(4) of heat-partition coefficient and contact temperatures for sliding semispaces with adhesion-deformational heat generation and contact heat exchange have been derived. On the basis of analytical study it has been established the following.

1. Heat partition depends on heat-generation configuration and contact heat exchange intensity on the transient interval $Fo \leq Fo_s$, while at $Fo > Fo_s$ it occurs due to thermal-effusivities proportion.
2. At low Fo numbers, contact temperatures rise as Fo for pure deformational heat generation and as \sqrt{Fo} in the presence of adhesive heat generation.
3. Under adhesion-deformational heat generation, perfect thermal contact is accompanied by variation of heat partition in time due to Eq.(11).
4. Heat flow at the surface of a semispace, sliding over a constant-temperature semispace, changes its direction at $Fo = Fo_c$.
5. For a semispace, sliding over a constant-temperature semispace, the ratio of the rates of adhesive and deformational heat generation has a noticeable influence on contact temperature on the interval $Fo \leq Fo_0$.

Acknowledgement

The author is obliged to Prof. Sato, Saitama University, for the valuable discussions on the principal points.

References

- [1] H. Blok, Theoretical study of temperature rise at surfaces of actual contact under oiliness lubricating conditions, General Discussion on Lubrication, Institution of Mechanical Engineers, London, 1937, vol.2, pp.222–235.
- [2] J. C. Jaeger, Moving sources of heat and the temperature of sliding contacts, Proceedings of the Royal Society of New South Wales 76 (1942) 203–224.
- [3] J. F. Archard, The temperature of rubbing surfaces, Wear 2 (6) (1958/59) 438–455.
- [4] H. S. Carslaw, J. C. Jaeger, Conduction of heat in solids, second ed., Oxford University Press, London, 1959, pp.87–89, pp.494–496.
- [5] F. F. Ling, T. E. Simkins, Measurement of pointwise juncture condition of temperature at the interface of two bodies in sliding contact, Journal of Basic Engineering 85 (1963) 481–487.
- [6] Ya. S. Podstrigach, The temperature field in a system of rigid bodies coupled by thin interface, Journal of Engineering Physics 6 (10) (1963) 129–136. (in Russian)

- [7] V. A. Balakin, Formation and distribution of heat in the frictional contact zone under conditions of non-stationary heat exchange, *Wear* 72 (2) (1981) 133–141.
- [8] I. V. Kragelskii, *Friction and Wear*, Butterworths, London, 1965.
- [9] B. V. Protasov, I. V. Kragelskii, On heat generation in external friction, *Journal of Friction and Wear* 2 (1982) 1–6.
- [10] F. E. Kennedy, Thermal and thermomechanical effects in dry sliding, *Wear* 100 (1984) 453–476.
- [11] J. H. Dautzenberg, J. H. Zaat, Quantitative determination of deformation by sliding wear, *Wear* 23 (1) (1973) 9–19.
- [12] M. A. Moore, R. M. Douthwaite, Plastic deformation below worn surfaces, *Metallurgical Transactions A* 7A (1976) 1833–1839.
- [13] P. Heilmann, D. A. Rigney, An energy-based model of friction and its application to coated systems, *Wear* 72 (2) (1981) 195–217.
- [14] F. E. Kennedy, Single pass rub phenomena — analysis and experiment, *Journal of Lubrication Technology* 104 (1982) 582–588.
- [15] D. A. Rigney, Transfer, mixing and associated chemical and mechanical processes during the sliding of ductile materials, *Wear* 245 (2000) 1–9.
- [16] B. V. Protasov, Energy proportions in a tribosystem and prognostication of its service durability, Saratov University Publisher, Saratov, 1979, pp. 32–73. (in Russian)
- [17] J. P. Bardon, Bases physiques des conditions de contact thermique imparfait entre milieux en glissement relatif, *Revue Générale de Thermique* 386 (1994) 85–92.
- [18] D. V. Grilitskii, Thermoelastic contact problems in tribology, Institute of topics and methods of teaching, Kyiv, 1996, pp. 70–92. (in Ukrainian)
- [19] P. P. Krasnyuk, Quasistatic contact interaction of two layers with heat generation caused by friction, *Material Science* 35 (2) (1999) 180–192.
- [20] N. S. Belyakov, A. P. Nosko, Mathematical simulation of thermal friction processes under conditions of nonideal contact, *High Temperature* 47 (1) (2009) 123–130.
- [21] N. S. Belyakov, A. P. Nosko, Thermoelastic problem of friction of plane-parallel layers with allowance for nonstationarity of thermal processes, *Journal of Friction and Wear* 31 (5) (2010) 317–325.
- [22] A. A. Yevtushenko, M. Kuciej, Influence of the convective cooling and the thermal resistance on the temperature of the pad/disc tribosystem, *International Communications in Heat and Mass Transfer* 37 (4) (2010) 337–342.
- [23] Y. C. Yang, H. L. Lee, W. L. Chen, J. L. Salazar, Estimation of thermal contact resistance and temperature distributions in the pad/disc tribosystem, *International Communications in Heat and Mass Transfer* 38 (3) (2011) 298–303.
- [24] A. A. Yevtushenko, M. Kuciej, The thermal problem of friction for a three-element tribosystem with composite strip, *International Journal of Heat and Mass Transfer* 54 (5) (2011) 5427–5437.
- [25] S. Malkin, A. Marmur, Temperatures in sliding and machining processes with distributed heat sources in the subsurface, *Wear* 42 (2) (1977) 333–340.
- [26] E. S. Sproles, D. J. Duquette, Interface temperature measurements in the fretting of a medium carbon steel, *Wear* 47 (2) (1978) 387–396.
- [27] V. A. Balakin, Heat-flow distribution and combined heat-mass transfer processes at the contact interface of a friction pair, *Journal of Engineering Physics* 40 (6) (1981) 660–665.
- [28] J. R. Barber, The conduction of heat from sliding solids, *International Journal of Heat and Mass Transfer* 13 (5) (1970) 857–869.
- [29] G. A. Berry, J. R. Barber, The division of frictional heat — a guide to the nature of sliding contact, *Journal of Tribology* 106 (1984) 405–415.
- [30] P. Chantrenne, M. Raynaud, A microscopic thermal model for dry sliding contact, *International Journal of Heat and Mass Transfer* 40 (5) (1997) 1083–1094.
- [31] P. Chantrenne, M. Raynaud, Study of a macroscopic sliding contact thermal model from microscopic models, *International Journal of Thermal Sciences* 40 (2001) 603–621.
- [32] F. F. Ling, S. L. Pu, Probable interface temperatures of solids in sliding contact, *Wear* 7 (1) (1964) 23–34.
- [33] L. Rozeanu, D. Pnueli, Two temperature gradients model for friction failure, *Journal of Lubrication Technology* 100 (1978) 479–485.
- [34] L. Rozeanu, D. Pnueli, Hardness controlled thermal failures, *Journal of Lubrication Technology* 102 (1980) 545–551.

List of figure captions

Fig.1. Boundary thermal conditions at sliding interface:

- (a) heat partition α_f ;
- (b) perfect thermal contact;
- (c) contact heat exchange;
- (d) partition α of heat-generation rate and contact heat exchange;
- (e) heat partition with account for microscopic thermal resistances R_i ;
- (f) adhesion-deformational heat generation and contact heat exchange

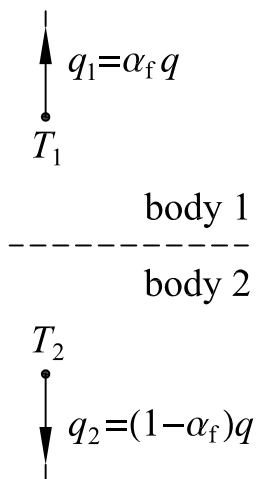
Fig.2. Typical profile of plastic displacement δ

Fig.3. Evolutions of J/α and α_f/α in relation to ψ_1 at $B \rightarrow 1$

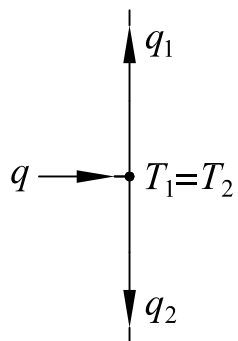
Fig.4. Relation between Fo_c and ψ_1 at various B

Fig.5. Evolution of θ_1/α in relation to ψ_1 at $B \rightarrow 1$

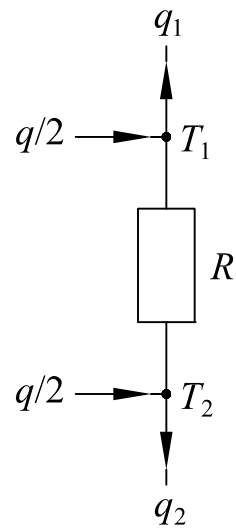
Fig.6. Variation range of ε



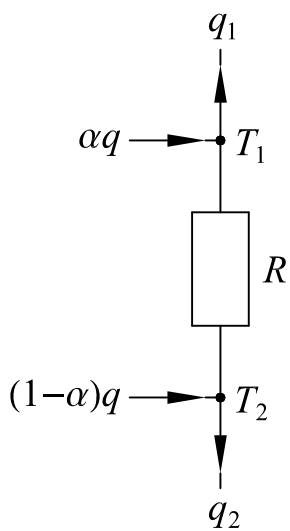
(a)



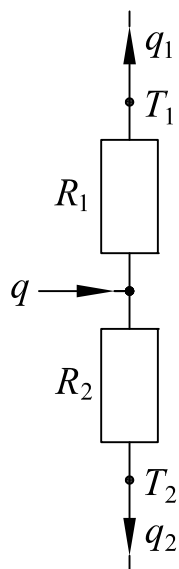
(b)



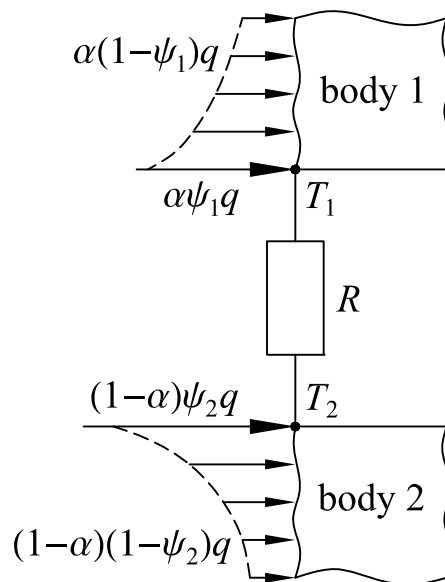
(c)



(d)



(e)



(f)

